2010 Digital Image Computing: Techniques and Applications

Reduction of Colour Artifacts using Inverse Demosaicking

Jim S. Jimmy Li and Sharmil Randhawa
School of Computer Science, Engineering and Mathematics
Flinders University, Australia
jimmy.li@flinders.edu.au, sharmil.randhawa@flinders.edu.au

Abstract

Most digital cameras use a single image sensor to capture colour images. As a result, only one colour at each pixel location is acquired. Demosaicking is a technique to estimate all the other missing colour pixel information in order to produce a full colour image, while inverse demosaicking refers to the recovery of the single image sensor values from the full colour image. Early digital cameras using primitive demosaicking algorithms to produce a full colour image have resulted in inferior quality images with colour artifacts. Generally, the removal of those artifacts is not achievable by the application of direct filtering. If we can recover the actual image sensor values from a full colour image and re-demosaic it again using state-of-the-art recently developed demosaicking algorithms, a better image can be produced without filtering. In this paper, a novel technique using wavelet transform is proposed to inverse demosaic a full colour image in order to recover the actual sensor values. It is then re-demosaicked using an advanced recently developed demosaicking method to reproduce an output image with minimal colour artifacts.

1. Introduction

Since the image sensor is the most expensive component of the digital camera [10], current consumer digital cameras use only a single CCD sensor to capture images. CCD image sensors can only detect information about the brightness of incident light, and thus a mosaic of colour filters is overlaid on the sensor to obtain colour information. However, each colour filter only passes one colour component.

The Bayer RGB pattern [1], shown in Fig. 1, is the most common colour filter array (CFA) used. The Bayer array measures the green colour on a quincunx (checkerboard) grid and the red and blue colours on rectangular grids. The green colour is sampled at twice the rate of the red or blue values because the peak sensitivity of the human visual system lies in the green spectrum [1]. The pattern exploits the fact that the human eye perceives intensity edges better than colour edges and that the green component contains the highest amount of intensity information [11].

CFA demosaicking is a digital process to obtain full colour images from images captured by a single image sensor. A Bayer mosaic image sensor does not allow the full red, green and blue colour planes to be captured. In other words, the image colour is captured in a sub-sampled pattern. Thus, in order to produce a full colour image, the missing colours at each pixel location must be interpolated.

Demosaicking refers to the estimation of the missing colour values in the CFA sensor data, and it is a critical process in the quality of the stored image. A majority of the cameras and cell phones will store images in the JPEG format (rather than RAW format), with the exception of professional digital cameras. For images captured by early generation digital cameras and digital cameras with limited computational capability, only simple demosaicking algorithms are implemented. Those simple demosaicking algorithms have a common problem in that they produce images with a significant amount of colour artifacts. These colour artifacts are generally difficult to be removed by filtering as they do not exhibit common noise characteristics.

With the advancement in the development of demosaicking algorithms [4, 9, 5, 8, 2, 13, 7], high quality images with minimal artifacts can be produced. In this paper, we propose to take advantage of this new development to re-demosaicked older images with colour artifacts which were previously produced by inferior primitive demosaicking techniques.

The quality of demosaicking algorithms impacts greatly on the amount of detail and artifacts seen in the processed digital images. When an image has fine details near the the resolution limit of the digital camera, the demosaicking algorithm can sometime produce false colour or colour moire patterns. Another artifact is the zipper effect which can usually be seen along abrupt edges.

One common feature of simple demosaicking algorithms to reduce computational burden is that they only process the missing colour values whilst leaving the original sensor data intact. Our proposed method is to extract those original

978-0-7695-4271-3/10 $26.00 © 2010 IEEE
DOI 10.1109/DICTA.2010.27

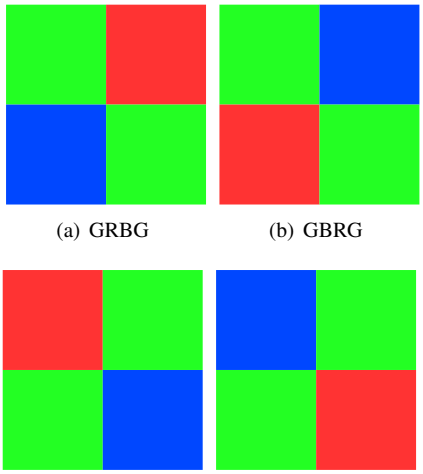

(a) GRBG (b) GBRG

(c) RGGB (d) BGGR

Figure 1. The 4 Possible Bayer Pattern Configurations.

sensor data from the full colour image for re-demosaicking using state-of-the-art demosaicking algorithms [4, 9, 5, 8, 2, 13, 7].

In section 2, we propose an inverse demosaicking technique to first extract the original CFA sensor data from the stored full colour image based on the assumption that the CFA sensor data remains more-or-less intact in the image processed by the simple demosaicking technique implemented in the digital camera. Section 3 gives a description of our overall proposed re-demosaicking method.

2. Extraction of True Colour Sensor Data

In this paper, we assume that the CFA pattern used is the Bayer pattern, but our proposed theory is applicable to other patterns. For the Bayer pattern, 50% of the pixels are green, 25% are red and 25% are blue. For the green pixels, they are located on a checkerboard grid, hence there are only four possible configurations as shown in Fig. 1. The first task for inverse demosaicking is to identify which one of the four CFA configurations was used in capturing the image. The subsequent task is to extract the CFA pixel values from the demosaicked image.

2.1. Assumptions for Inverse Demosaicking

Our proposed method is based on the following assumptions.

2.1.1 Assumption 1

For simple demosaicking algorithms used in the early generation digital cameras, the CFA pixel values from the sensor before demosaicking will more-or-less be retained after demosaicking, i.e. the simple demosaicking process will not alter those sensor pixel values, and will only interpolate the other missing colour pixel values. The reason was to reduce computational burden of the demosaicking process because the computational capability of the early generation cameras was very limited. Moreover since those sensor pixel values are the actual true values, it is rational and practical to retain those values in the demosaicked image.

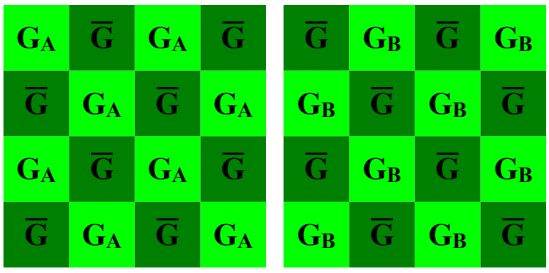

(a) The green plane with G_A as the true sensor values, as indicated in Fig. 1(a) and Fig. 1(b). (b) The green plane with G_B as the true sensor values, as indicated in Fig. 1(c) and Fig. 1(d).

Figure 2. Alternatives for Actual Green Pixel Location.

2.1.2 Assumption 2

Since the missing pixel values are generally determined by interpolating neighbourhood values by some form of averaging techniques such as Bilinear and Freeman [3], they are usually smoother than the actual sensor values. In other words, the interpolated pixel values will contain less high frequency component energy than the actual sensor pixel values.

Both assumptions were experimentally verified and the results are presented in the next section in this paper.

2.2. Location of True Green Sensor Pixels

After demosaicking, half of the green plane pixels consist of true green sensor values, and the other half are interpolated values. According to Fig. 1, the two possible locations of the true green sensor values, namely G_A and G_B, are shown in Fig. 2, where G represents the actual green pixel values and $\overline{G}$ represents the interpolated green pixel values.

For each alternative in Fig. 2, the green plane is divided into two sub-images of green pixels as shown in Fig. 3, so that one sub-image contains only actual green sensor values, and the other contains only interpolated green values.

In order to identify the sub-image containing the actual green values, we examine their high frequency component energy. Based on Assumption 2 in section 2.1.2 that the interpolated green values $\overline{G}$ are smoother than the actual green CFA data, the sub-image which contains more high frequency component energy is the one which contains only actual green sensor values.

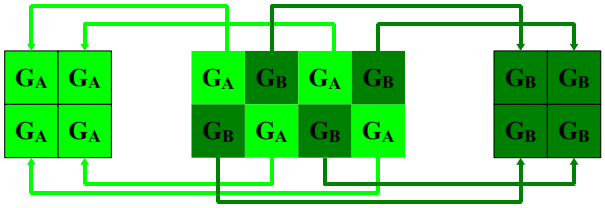

Figure 3. Extraction of Green pixels to form G_A and G_B sub-images.

In order to compare the energy levels of the high frequency components between the two sub-images, we use filter banks to perform an undecimated wavelet transform. The filter bank structure consists of 2D seperable filters constructed from a low-pass filter (1) and a high-pass filter (2) to decompose each sub-images into 4 subbands, namely (LL) both rows and columns are low-pass, filtered, (LH) rows are low-pass filtered, columns are high-pass filtered, (HL) rows are high-pass filtered, columns are low-pass filtered, (HH) both rows and columns are high-pass filtered.

$$h_0 = [1\ 2\ 1]/4 \tag{1}$$

$$h_1 = [1\ -2\ 1]/4 \tag{2}$$

The four subbands of a sub-image $G(m,n)$ are determined as follows:

$$LL(m,n) = h_0(m) * [h_0(n) * G(m,n)] \tag{3}$$

$$LH(m,n) = h_0(m) * [h_1(n) * G(m,n)] \tag{4}$$

$$HL(m,n) = h_1(m) * [h_0(n) * G(m,n)] \tag{5}$$

$$HH(m,n) = h_1(m) * [h_1(n) * G(m,n)] \tag{6}$$

Since the HH subband represents the quantity of only high frequency energy, we compare the HH subband for each sub-image and the one with the higher energy value is the sub-image that contains only actual sensor values.

Let E be the total energy for the high frequency components for the HH subband.

$$E = \sum_{m,n} HH(m,n)^2 \tag{7}$$

where m, n are the spatial coordinates of the HH subband.

2.3. Location of True Red and Blue Sensor Pixels

Once the true green pixel location is confirmed, the remaining task is to identify the actual red and blue sensor pixel locations. If the G_A sub-image is chosen, the possible CFA configurations are those shown in Fig. 1(a) and 1(b). Otherwise, if the G_B sub-image is chosen instead, the other two possible configurations are those shown in Fig. 1(c) and 1(d).

Without loss of generality, we suppose that the G_A sub-image indicates the true location for the green pixels. As a result, the only two possible configurations for the red and blue pixel locations are shown by Fig. 1(a) and Fig. 1(b). The next task is to identify which of the above two is the correct configuration. To determine the energy level of the high frequency component for the red pixels, we extract the red pixels to produce a down-sampled red plane, as shown in Fig. 4(a) and then apply (6)-(7) to determine the total energy, E_{Red}. A similar process is applied to determine the energy level of the high frequency component for the blue pixels E_{Blue}. Let E_{RB} be the total energy for the red and blue down-sampled planes.

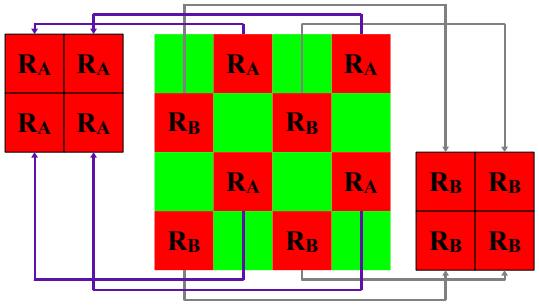

(a) Extraction of Red pixels to form R_1 and R_2 sub-images.

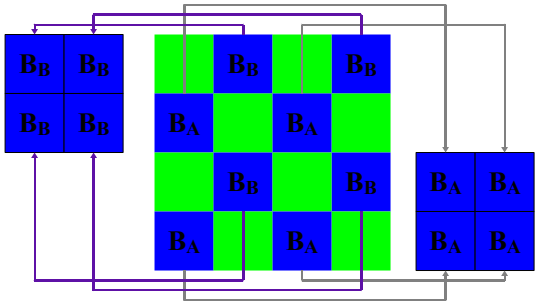

(b) Extraction of Blue pixels to form B_1 and B_2 sub-images.

Figure 4. Extraction of Red and Blue sub-images.

$$E_{RB} = E_{Red} + E_{Blue} \tag{8}$$

The E_{RB} for each configuration is then evaluated and compared, and the configuration with the higher E_{RB} is considered to be the correct one.

3. Our Proposed Method

Once the configuration of the Bayer pattern is determined, the actual CFA sensor data can now be extracted from the full colour demosaicked image. A state-of-the-art demosaicking algorithm can now be applied to the CFA data for re-demosaicking. For experimental purposes, the demosaicking method described in [14] was applied. This recently developed demosaicking technique can produce a demosaicked colour image with minimal colour artifacts whilst preserving sharp colour edges.

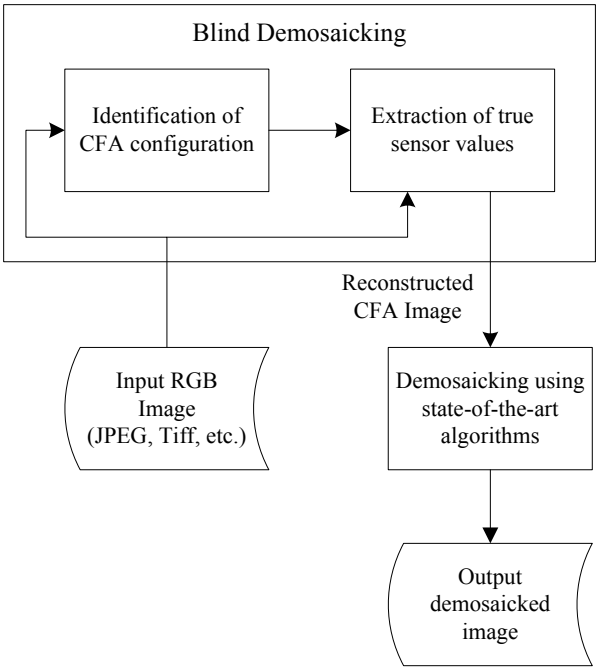

Figure 5. Block Diagram of Our Proposed Method.

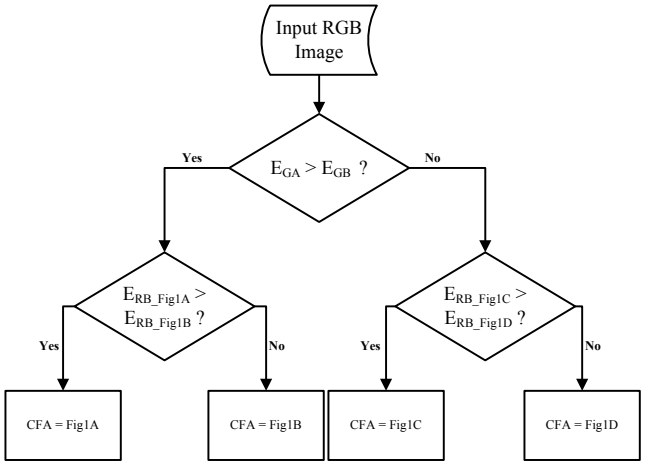

Figure 6. Identification of CFA Configuration.

The block diagram of our proposed method is shown in Fig. 5. The input colour image with colour artifacts is first analysed to identify the actual CFA Bayer pattern in the camera used to capture the original image. Fig. 6 gives the flowchart for the identification process. Once the CFA configuration is identified, the original CFA is re-constructed from the full-colour image. This re-constructed CFA is then demosaicked using state-of-the-art algorithms with minimal colour artifacts.

Figure 7. Test Images 7(a)-(t) from left to right, top to bottom.

4. Experimental Results

For experimental assessment, we assumed that early generation digital cameras used one of the two simple demosaicking techniques, namely Bilinear and Freeman [3], and the output is a demosaicked full colour image. If the input is in JPEG format, it will first be decompressed to give a full colour image.

To assess the performance of our proposed method for images with different characteristics, twenty standard test images [6] as shown in Fig. 7 were used. These test images were first used to generate a set of CFA Bayer images with various configurations as shown in Fig. 1. They were then demosaicked using two chosen simple demosaicking methods, namely Bilinear and Freeman [3]. After the application of our proposed re-demosaicking method, the results are tabulated in Table 1, which gives the Peak Signal-to-Noise Ratio (PSNR) [2] and the Normalized Color Difference (NCD) [12] quality measures. This confirms that our proposed method produced a re-demosaicked image with a quality higher than its input. From our experimental results, our inverse demosaicking method can correctly identify all the actual CFA Bayer configuration without errors.

For visual assessment, we used Fig. 8(a) which is a section in Fig. 7(q) for evaluation. This section contains the mast of a boat showing thin wires which cause problems to many demosaicking algorithms resulting in the production of colour artifacts. Fig. 8(b) is a demosaicked image using Bilinear and Fig. 8(c) is demosaicked by Freeman. Both figures clearly contain ample visual colour artifacts around that mast region. The output produced by our proposed re-demosaicking algorithm, as shown in Fig. 8(d), has clearly resulted in less colour artifacts. The quality of the output is now comparable to that of a contemporary digital camera using state-of-the-art demosaicking algorithms. To further evaluate our method visually, we applied our proposed re-demosaicking method to another image with different features as shown in Fig. 9. The output image produced by our proposed re-demosaicking method confirms

that our method can reproduce an image with higher quality than the original full colour image. Moreover, this confirms that images not in RAW format (digital negative) can still be re-demosaicked to produce better quality images.

5. Conclusion

It is always desirable to make use of the advancement of new research to produce better results. This is exactly the idea of our proposal to improve the quality of older images taken by early generation digital cameras using the advancement of demosaicking algorithms. As most amateur digital cameras store their images in non-Raw (non-digital negative) format, colour artifacts are generally difficult to remove by direct application of filtering. Our proposed method using inverse demosaicking avoids the requirement of an input image being in digital negative (RAW) format and allows images in any format to be re-demosaicked in order to produce a higher quality image. It has been shown that our proposed inverse demosaicking method using wavelet transform can successful identity the CFA Bayer pattern used in the digital camera sensor. All-in-all our proposed method is able to improve and reduce colour artifacts for digital images taken by early generation digital cameras and can also be applied in the future to improve digital images when better demosaicking methods have been developed.

References

[1] B. E. Bayer. Color imaging array. *US Patent 3 971 065*, 1976. 1

[2] K.-H. Chung and Y.-H. Chan. Color demosaicing using variance of color differences. *IEEE Transactions on Image Processing*, 15(10):2944–2955, 2006. 1, 2, 4

[3] W. Freeman. Median filter for reconstructing missing color samples. *US Patent 4,724,395*, 1988. 2, 4

[4] B. K. Gunturk, Y. Altunbasak, and R. M. Mersereau. Color plane interpolation using alternating projections. *IEEE Transactions on Image Processing*, 11(9):997–1013, 2002. 1, 2

[5] K. Hirakawa and T. W. Parks. Adaptive homogeneity-directed demosaicing algorithm. *IEEE Transactions on Image Processing*, 14(3):360–369, March 2005. 1, 2

[6] Kodak. Kodak true color image collection. `http://r0k.us/graphics/kodak/`. 4

[7] J. S. J. Li and S. Randhawa. Color filter array demosaicking using high order interpolation techniques with a weighted median filter for sharp color edge preservation. *IEEE Transactions on Image Processing*, 18(9):1946–1957, 2009. 1, 2

[8] X. Li. Demosaicing by successive approximation. *IEEE Transactions on Image Processing*, 14(3):370–379, 2005. 1, 2

[9] W. Lu and Y.-P. Tan. Color filter array demosaicking: New method and performance measures. *IEEE Transactions on Image Processing*, 12(10):1194–1210, 2003. 1, 2

(a) Original Image

(b) Bilinear

(c) Freeman

(d) Our Proposed Method

Figure 8. Mast of boat of (a) Original image in Fig. 7(q) and the demosaicked output images using (b) Bilinear interpolation, (c) Freeman and (d) Our Proposed Method.

[10] R. Lukac, editor. *Single-Sensor Imaging: Methods and Applications for Digital Cameras*. CRC Press, 2008. 1

[11] S. Neter. Methods and systems for detecting defective imag-

(a) Original Image (b) Bilinear

(c) Freeman (d) Our Proposed Method

Figure 9. Words in (a) Original image and the demosaicked output images using (b) Bilinear interpolation, (c) Freeman and (d) Our Proposed Method.

Table 1. Image Quality Performance Measures - PSNR and NCD ($\times 10^{-3}$).

Methods:	**Bilinear**	**Freeman**	**Proposed Method**	**Bilinear**	**Freeman**	**Proposed Method**
Images	**PSNR**			**NCD**		
Fig. 7(a)	26.37	32.13	38.53	93.93	53.95	27.99
Fig. 7(b)	33.16	38.10	40.92	48.55	31.70	24.62
Fig. 7(c)	26.71	34.19	38.13	110.24	58.62	40.80
Fig. 7(d)	27.85	33.51	40.30	60.96	34.52	17.77
Fig. 7(e)	33.54	40.20	42.40	38.57	22.77	18.87
Fig. 7(f)	23.58	28.61	36.11	94.66	57.03	28.14
Fig. 7(g)	32.49	38.18	42.90	25.69	15.73	10.78
Fig. 7(h)	32.51	38.94	42.61	24.49	14.14	10.60
Fig. 7(i)	29.18	35.17	40.13	75.74	44.29	26.23
Fig. 7(j)	33.54	39.00	43.55	23.22	14.15	9.64
Fig. 7(k)	23.89	30.38	34.84	129.40	70.06	44.05
Fig. 7(l)	33.06	38.36	39.88	44.46	29.56	25.63
Fig. 7(m)	31.35	36.71	43.86	51.04	30.55	15.15
Fig. 7(n)	32.18	38.83	41.91	65.21	39.15	30.50
Fig. 7(o)	28.10	34.21	37.37	100.87	58.10	45.20
Fig. 7(p)	28.10	33.43	40.92	67.01	39.12	21.27
Fig. 7(q)	31.63	37.90	41.26	36.06	22.22	16.66
Fig. 7(r)	28.53	34.45	39.21	60.86	34.90	21.31
Fig. 7(s)	30.42	35.50	38.51	54.42	33.79	26.55
Fig. 7(t)	26.74	32.37	35.50	72.03	42.01	29.53

ing pixels and pixel values. *US Patent 6,965,395 B1*, 2005. 1

[12] K. N. Plataniotis and A. N. Venetsanopoulos. *Color Image Processing and Applications*. Springer Verlag, 2000. 4

[13] X. L. Wu and L. Zhang. Improvement of color video demosaicking in temporal domain. *IEEE Transactions on Image Processing*, 15(10):3138–3151, October 2006. 1, 2

[14] L. Zhang and X. L. Wu. Color demosaicking via directional linear minimum mean square-error estimation. 14(12):2167–2178, December 2005. 3